Numerical Analysis of the Dependence of the Thrust Performance on the Configuration in a Miniature Microwave Discharge Thruster

IEPC-2017-324

Presented at the 35th International Electric Propulsion Conference
Georgia Institute of Technology • Atlanta, Georgia • USA
October 8 – 12, 2017

Koichi Ushio,[1] Tomoki Koyama,[2] Bunsuke Ueno,[3] Taichi Morita,[4] Naoji Yamamoto[5] and Hideki Nakashima[6]
Kyushu University, Kasuga, Fukuoka, 816-8580, Japan

Abstract: **A miniature microwave discharge plasma thruster for microsatellites is under development, with the target power consumption, thrust and specific impulse of 10 W, 1 mN and 1000 sec, respectively. Previous research revealed that the performance of the thruster doesn't achieve the objective performance. It is necessary to understand the physical phenomenon in the discharge chamber. Therefore, we developed the numerical code using Finite-Difference Time-Domain method and Particle in Cell method and analyzed the dependence of the electron heating on the antenna configuration. Results showed electrons are heated near the antenna and high energized electrons diffuse along the magnetic field line. Results also indicate that electron could be energized sufficiently to ionize neutral particle without a round trip along the magnetic field line.**

Nomenclature

E	=	electric field
H	=	magnetic field
J	=	current density
μ_0	=	permeability in a vacuum
ε_0	=	permittivity in a vacuum
m	=	mass of electron
v	=	velocity of electron
e	=	elementary charge

I. Introduction

THE number of launch of microsatellites (under 100 kg) is increasing,[1] since microsatellite is low cost and developed in short period. The market of the microsatellites and nanosatellites will grow up in the future.[2] Due to the limitation of space and power, only a few microsatellites have propulsion system.[3,4] Therefore, a lot of miniature thrusters for microsatellites are under development.[5-9] We also have been developing 1 mN class thrust system at the power consumption of under 30 W for various applications.[10] Figure 1 shows the parts assembly of the thruster. Sm-Co magnets surround the discharge chamber which are located between yokes made of soft iron. Antenna for

[1] 2nd grade Doctoral student, Department of Advanced Energy Engineering Science, ushio@aees.kyushu-u.ac.jp
[2] Graduated student, Department of Advanced Energy Engineering Science, tomoki@aees.kyushu-u.ac.jp
[3] Graduated student, Department of Advanced Energy Engineering Science, b-ueno@aees.kyushu-u.ac.jp
[4] Assistant professor, Department of Advanced Energy Engineering Science, morita@aees.kyushu-u.ac.jp
[5] Professor, Department of Advanced Energy Engineering Science, yamamoto@aees.kyushu-u.ac.jp
[6] Emeritus Professor, Department of Advanced Energy Engineering Science, nakasima@aees.kyushu-u.ac.jp

microwave discharge is located at the center of the discharge chamber. In this thruster, the plasma is generated by microwave discharge and extracted by the potential difference between the plasma potential in the discharge chamber and space potential with keeping electrical neutrality. The subsystems for this thruster are only microwave power supply and propellant feeding system, so this thruster realize a simple thruster system. In previous research, we investigated the dependence of ion beam current on the thruster configuration including the antenna configuration, magnetic field shape and the length of the discharge chamber.[11] Figure 2 shows the photos of the three types of antenna; (a)L shape, (b)small disk and (c)disk. As a result, we obtained the ion beam current as shown in Fig.3. As shown in this figure, the small disk antenna showed the best performance, with the disk antenna showing the next best performance. The ion beam current with the L shaped antenna was very low (1~2 mA). However, the thrust performance is not enough to achieve the objective performance even if small disk antenna is adopted and it is unclear how these configurations affect the thrust performance.[12] Therefore, we developed the numerical code by coupling Finite-Difference Time-Domain(FDTD) method and Particle in Cell(PIC) method simulating the plasma generation to optimize the thruster configuration efficiently. PIC method can treat movement of electrons, collision process and energy distribution function while FDTD method can analyze absorption of microwave in plasma. In fact, this coupling code is just a portion of the numerical simulation code to obtain steady state. This numerical simulation code has been developing for microwave discharge neutralizer under development in Kyushu university.[13] This codes is composed of the FDTD-PIC code which calculate the electron heating by the microwave and Full-PIC code which calculate the motion of the particle and electrostatic field. In Full-PIC code, Both of ions and electrons is treated as a particle, so we can solve Poisson's equation. Energy gain probability distribution function calculated in FDTD-PIC is passed to Full-PIC code to calculate the motion of the electrons and ions. In this paper, we discussed about how the antenna configuration affects the electron heating and plasma generation in FDTD-PIC code. Full-PIC code for our thruster is under development.

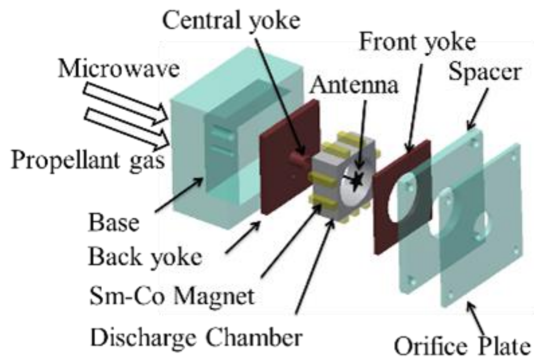

Figure 1. Parts assembly of the thruster.

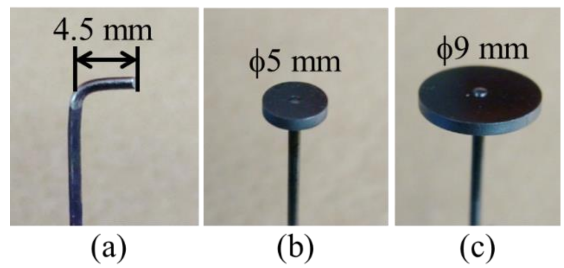

Figure 2. Appearance of antenna

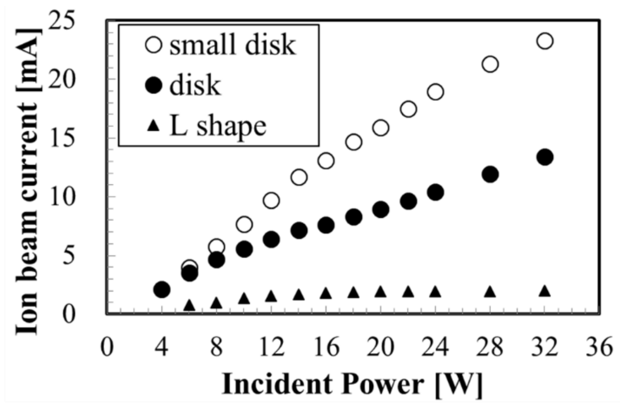

Figure 3. Ion beam current with each antenna

II. Calculation method

A. FDTD and PIC Method

The FDTD method is used to analyze the propagation of the microwave. The basic equation of FDTD method is Maxwell's equation as follows:

$$\nabla \times \boldsymbol{E} = -\mu_0 \frac{\partial \boldsymbol{H}}{\partial t} \qquad (1)$$

$$\nabla \times \boldsymbol{H} = \varepsilon_0 \frac{\partial \boldsymbol{E}}{\partial t} + \boldsymbol{J} \qquad (2)$$

where μ_0 and ε_0 are the permeability and permittivity in a vacuum. $\boldsymbol{E}$ and $\boldsymbol{H}$ is the electric field and the magnetic field of the microwave. $\boldsymbol{J}$ is the current density calculated from the motion of the electron in PIC method. This equation is solved by leap-frog method. In the FDTD method, electromagnetic fields are defined at the points half of the cell size away from grid points as suggested by Yee.[14] Microwave feeding is simulated by giving electric fields at the root of the antenna. The PIC method is used to analyze the motion of the electrons. The basic equation of the PIC method is the equation of motion as follows:

$$m\frac{d\boldsymbol{v}}{dt} = e(\boldsymbol{E} + \boldsymbol{v} \times \boldsymbol{B}) \tag{3}$$

where m, $\boldsymbol{v}$ and e are the mass, velocity and charge of the electron. $\boldsymbol{E}$ is the electric field calculated by FDTD method. $\boldsymbol{B}$ is the magnetic flux density generated by permanent magnet calculated by a software named Magnum(©Field precision). Magnetic field of the microwave is ignored in PIC method because the magnetic field of microwave is too small compared with the static magnetic field of permanent magnet. These field value is interpolated to particle linearly. Only collisions between electrons and neutral particles is considered by using the Monte Carlo method and Null-collision method.[15]

FDTD method and PIC method is coupled as shown in Fig.4. PIC method calculates the particle motion using electric field calculated by FDTD method. FDTD method calculate the microwave propagation considering particle motion by using the current density calculated by PIC method. Time evolution is solved by iterating this process. In this coupling calculation, steady state can't be obtained because the motion of the ion and the electrostatic field generated by non-uniform distribution of the charged particle isn't considered.

B. Boundary Conditions

Perfect Electrical Conductor(PEC) boundary condition is applied to all conductor in calculation area. Antenna is simulated by making electric field along the antenna zero. 1st Mur boundary condition is applied to the root of antenna to prevent the microwave reflecting. Electrons under 20 eV are reflected at the surface of the conductor to simulate the sheath.

C. Calculation Geometry and Parameters

In this code, 3D-cartesian coordinates is used and the lengths of the calculation area in the x-, y-, and z-directions are 20, 20, and 36 mm,

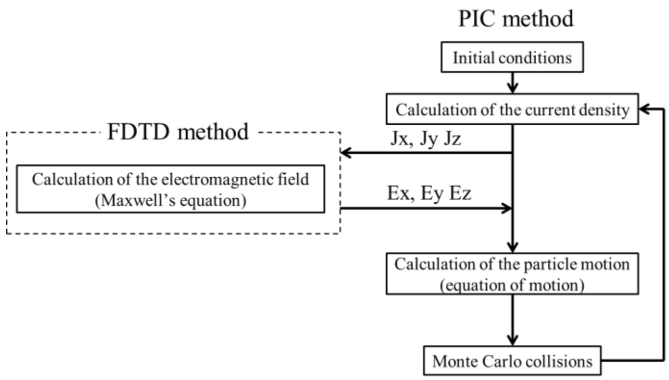

Figure 4. Flow chart of the code

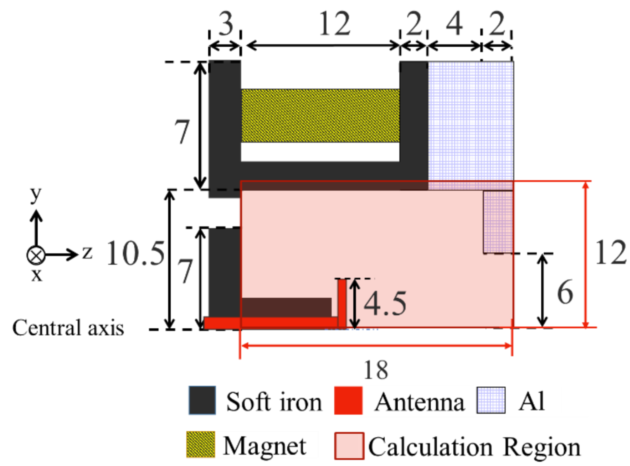

Figure 5. Calculation geometry

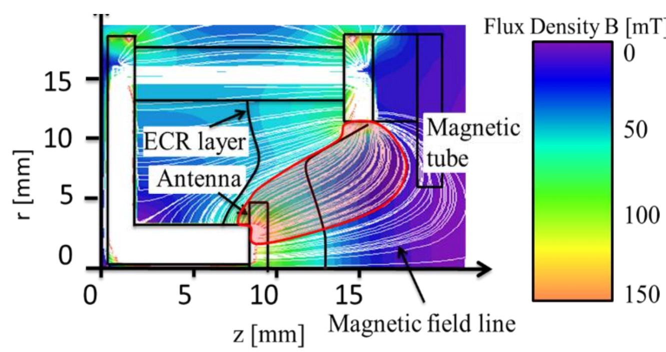

Figure 6. Magnet field distribution

Table 1. Calculation parameters

Time step (FDTD)	2.5×10^{-14} s
Time step (PIC)	2.5×10^{-13} s
Mesh size	5.0×10^{-4} m
Microwave frequency	1.6 GHz
Propellant	Argon
Density of the neutral particle	2.0×10^{20} m^{-3}(uniform)
Initial plasma density	1.0×10^{17} m^{-3}(uniform)
Initial electron temperature	2.0 eV
Input electric field	5.5×10^{4} V/m

respectively. Figure 5 shows the geometry of the calculation area. Figure 6 shows the magnet field distribution in the calculation area with 9 magnets. The number of magnets was optimized in previous research. In Fig.5, red area is called magnetic tube.[16] Electrons make a round trip in this area and they are energized by strong electric field near the antenna. Electron cyclotron resonance(ECR) layer shows the contour line whose magnetic field strength is 57.1 mT. It seemed that the ECR layer is also related with the electron heating.

Table 1 shows operation parameters and the calculation conditions. Operation parameters is same as previous experiments. Initial plasma density and initial electron energy are decided form the previous results measured by using Langmuir probe[17,18] and these are distributed uniformly. Input electric field was adjusted to make an electron absorption power in PIC method and net incident power in the experiments equal. Electron absorption power is calculated from the variation of the kinetic energy. Same electric field was fed to all antenna and electron absorption powers averaged over last 5 ns were 4.3 W, 18.6 W and 18 W with L shape antenna, small disk antenna and disk antenna, respectively. These absorption powers are almost equal to the power obtained by subtracting reflected power from input power in the experiments for disk and small disk antenna with 20 W forward incident power. On the other hand, absorption power with L shape antenna isn't equal to a net incident power in the experiment because L shape antenna needed a stub tuner to stabilize the plasma.

III. Results

Figure 7 and 8 shows the electric field distribution in x-y plane, y-z plane with (a) L shape, (b) small disk and (c) disk, respectively. As shown in these figures, strong electric field is generated only near the antenna surface. This thickness is much smaller than the skin depth($\cong$ 17 mm). This means that the discharge chamber is too small rather than the wavelength of microwave, so microwave couldn't propagate keeping waveform and we couldn't apply ordinary theory of skin effect. This tendency occurred when microwave was fed to small discharge chamber compared with wavelength by method like our thruster, so this tendency of the electric field is also observed in numerical analysis of the miniature microwave discharge thruster which has the 18 mm diameter discharge chamber and same microwave feeding method.[19] L shape antenna generate the strong electric field at the tip of the L shape. Small disk antenna generate the electric field around the antenna. On the other hand, disk antenna generate weak electric field around the edge of the disk. Note that the electric field at the positive z side of small disk antenna is stronger than the one with disk antenna. In addition, there is no strong electric field around ECR layer. As results, energized electrons are distributed as shown in Fig.9 and 10. Electrons near the tip or edge of the antenna are energized highly and diffuse along the magnetic field line shown in these figures. As a result, high energized electrons distribute along the magnetic field line. High energized electrons with L shape antenna distribute only in the positive y side. High energized electrons with small disk antenna and disk antenna distribute in whole of the magnetic tube. On the other hand, the electrons at the positive z side of the antenna is energized highly only with the small disk antenna. Figure 11 shows the distribution of the place of the ionization collision. These distributions correspond to the region of the high energized electrons. These results indicate that diffused electrons energized around the antenna not around the ECR layer cause ionization. This indication is same as the result of the numerical analysis for microwave discharge neutralizer.[20] Note that ionization is occurred in the positive z side of the antenna only when the small disk antenna was used. This mean that electrons can be energized sufficiently to ionize the neutral particle without round trip along the magnetic field line if there was a enough electric field like small antenna. This characteristics of the small disk antenna will affect the electron density distribution and potential in steady state, As a result, it seemed that the largest ion beam current was obtained. Next, we calculated the energy gain probability distribution function(EGDF). Two characteristic examples are shown in Fig.12 and Fig.13 at the positive z side of the antenna. This function was calculated from energy variation of electrons averaged over last 10 ns for each sells. In addition, this is averaged spatially in same radius from the central axis to be passed to 2D-Full-PIC code. As shown in Fig.12, EGDF at the tip of disk antenna has sharp peak at 0 eV. This is because most of the electrons aren't energized because there is no strong electric field with disk antenna at this area. On the other hand, EGDF with small disk has a wide distribution. This is because many electrons are energized or de-energized by wide electric field generated by small disk antenna. Certainly, EDGF reflecting the characteristics of electron heating with each antennas was obtained. In 2D-Full-PIC code, electrons are energized according to this probability function. Therefore, we will obtain the steady state reflecting the electric heating with each antenna.

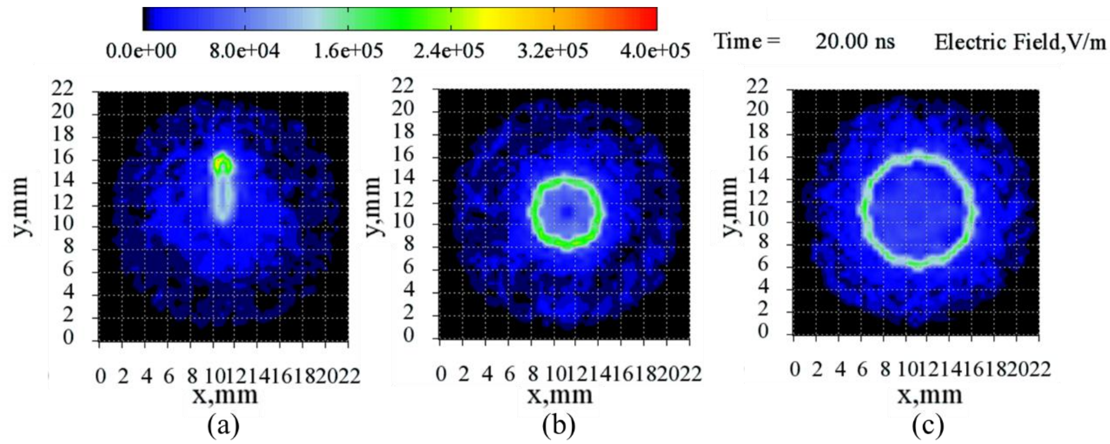

Figure 7. Electric field distribution on x-y plane. (a) L shape, (b) small disk, (c) disk

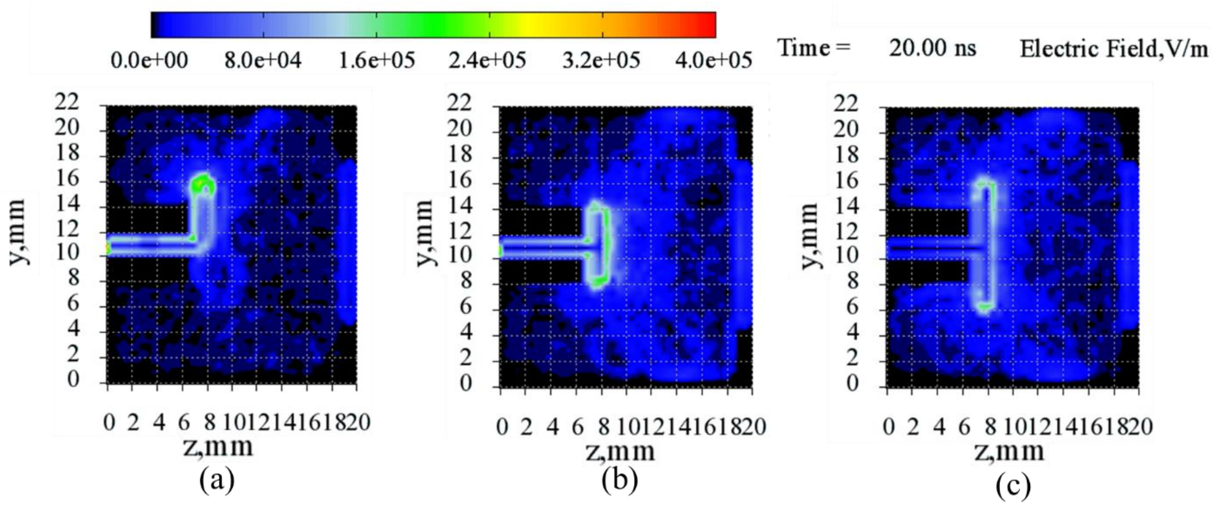

Figure 8. Electric field distribution on y-z plane. (a) L shape, (b) small disk, (c) disk

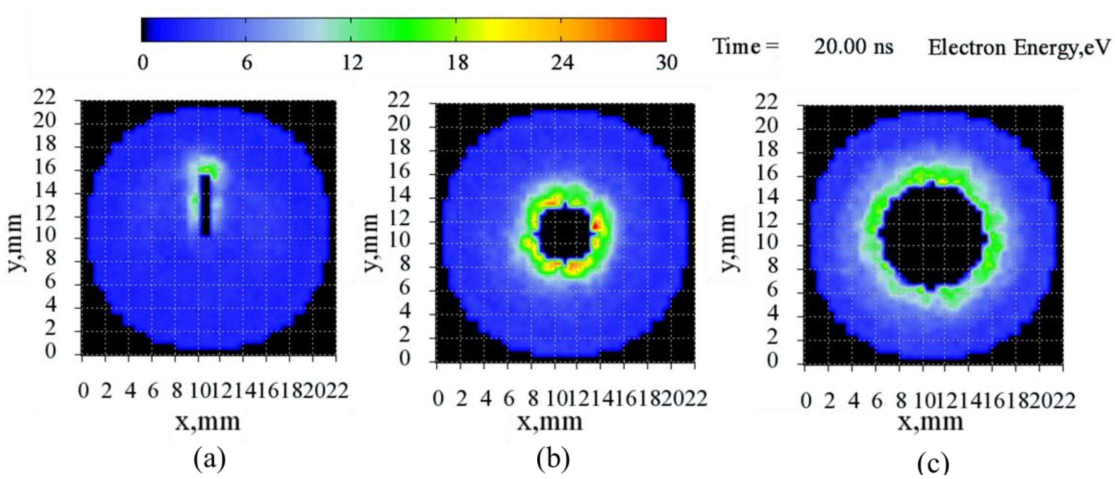

Figure 9. Electron energy distribution on x-y plane. (a) L shape, (b) small disk, (c) disk

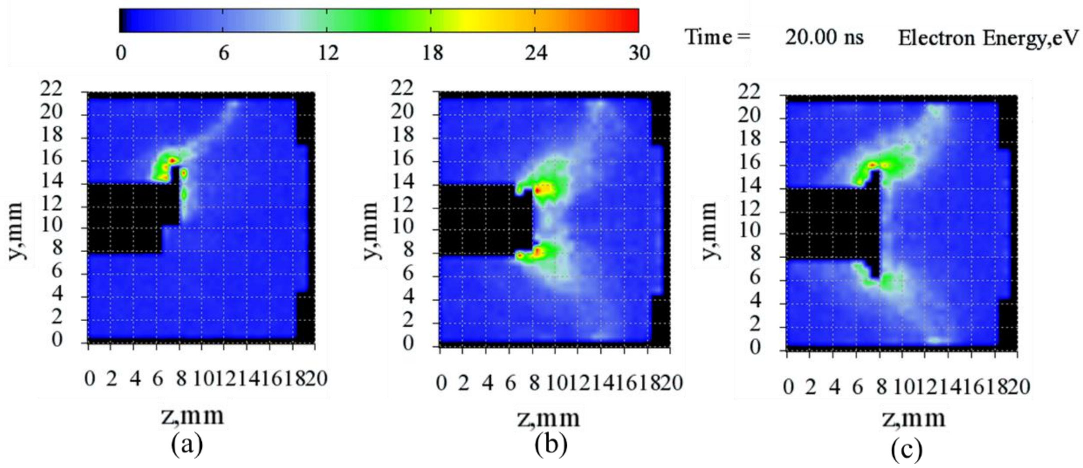

Figure 10. Electron energy distribution on y-z plane. (a) L shape, (b) small disk, (c) disk

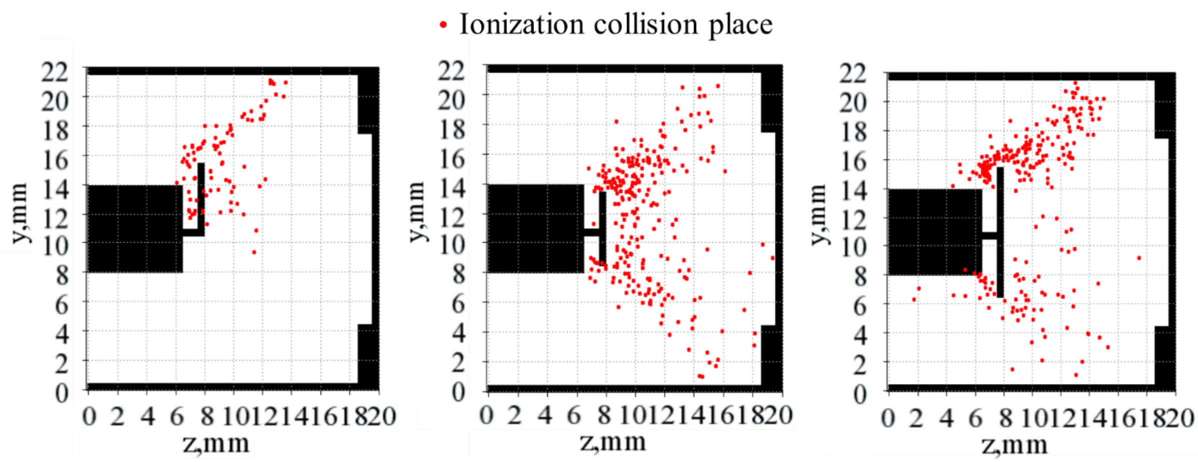

Figure 11. Distribution of the ionization place. (a) L shape, (b) small disk, (c) disk

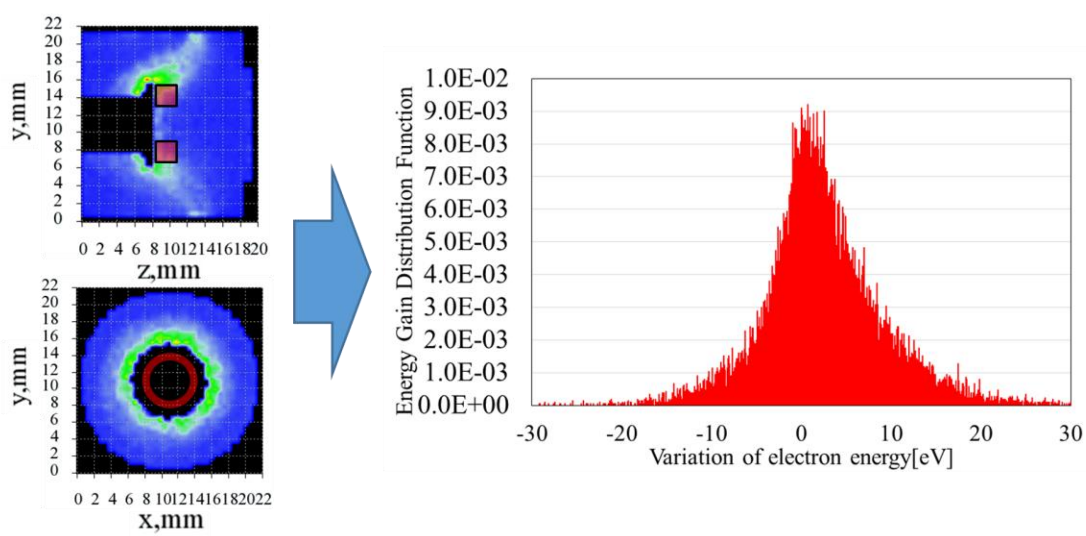

Figure 12. Energy gain distribution function with disk antenna

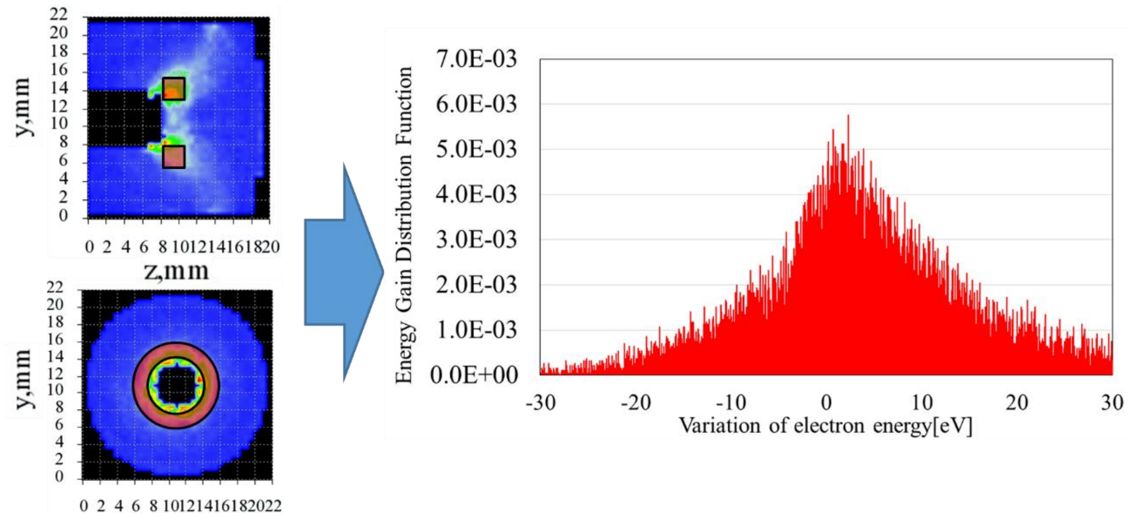

Figure 13. Energy gain distribution function with small disk antenna

IV. Conclusion

Three dimensional FDTD-PIC coupling code to simulate the electron heating in the miniature microwave discharge thruster was developed and the relationship between the configuration of antenna and electron heating was investigated. Three types of antenna; L shape antenna, small disk antenna and disk antenna was simulated. The results showed that electric field near the antenna energize the electrons mainly and energized electrons diffuse along the magnetic field line. It is indicated that electric field at the positive z side of small disk antenna has the important effect on the ion beam current. We also calculate the energy gain distribution probability function to couple this 3D-FDTD-PIC code and 2D-Full-PIC code. As a future work, we should couple this 3D-FDTD-PIC code and 2D-Full-PIC code considering the electrostatic field by solving Poisson's equation and obtain the steady state including the generation of the potential difference.

References

[1]King, P. J. and Bradford, A., "Launching the Small Satellite Revolution, Realising a reliable, cost effective and dedicated launch service", *Proceeding of 67th International Astronautical Congress*, IAC-16-B4.5.3, 2016

[2]Philip D., David R., Oliver T., Andy B. and Alex da S. C., "Vertical Launch of Small Satellites from the UK", *Proceeding of 67th International Astronautical Congress*, IAC-16-B4.5.5, 2016

[3]Tsuruda, Y., Nakasuka S., Matsui, M., Mase, I.: Reasonably Reliable System Design and Operation for Twin Satellite: Hodoyoshi-3 & 4, *Proceedings of 58th Space Sciences and Technology Conference*, Nov.2014 (in Japanese).

[4]Koizumi, H., Kasagi, Y., Inagaki, T., Kawahara, H, Yaginuma, K., Asakawa, J., Komurasaki, K.: Development of small propulsion system for nano-satellites and its challenges for the future, *Proceedings of 58th Space Sciences and Technology Conference*, Nov. 2014 (in Japanese)

[5]Greig, A., Charles, C., Boswell, W. R., "Spatiotemporal study of gas heating mechanisms in a radio frequency electrothermal plasma micro-thruster", *Frontiers in Physics*, Volume 3, id.84, 2015

[6]Ueno, K., Mori, D., Takao, Y., Eriguchi, K. and Ono, K., "Paticle-in-Cell Simulation of a Micro ECR Plasma Thruster", *Proceeding of Joint Conference of 30th International Symposium on Space Technology and Science, 34th International Electric Propulsion Conference and 6th Nano-satellite Symposium*, IEPC-2015-240, 2015

[7]Cannat, F., Jarrige, J., Lafleur, T., Elias, -Q. P. and Packan, D. "Experimental geometry investigation of a coaxial ECR plasma thruster" *Proceeding of Joint Conference of 30th International Symposium on Space Technology and Science, 34th International Electric Propulsion Conference and 6th Nano-satellite Symposium*, IEPC-2015-242, 2015

[8]J. P. Sheehan, Timothy A. Collard, Frans H. Ebersohn, and Benjamin W. Longmier, "Initial Operation of the CubeSat Ambipolar Thruster", *Proceeding of Joint Conference of 30th International Symposium on Space Technology and Science, 34th International Electric Propulsion Conference and 6th Nano-satellite Symposium*, IEPC-2015-243, 2015

[9]Biggs, D., Avery, S., Raymond, L., Liang, W., Gascon, N., Fabris L. A., Davila, R. J. and Cappelli, M., "A Compact Helicon Thruster for CubeSat Applications", *Proceeding of Joint Conference of 30th International Symposium on Space Technology and Science, 34th International Electric Propulsion Conference and 6th Nano-satellite Symposium*, IEPC-2015-244, 2015

[10]Toyoda, Y., Ushio, K., Yamamoto, N. and Nakashima, H.: Development of a Miniature Microwave Discharge Plasma Thruster, Journal of IAPS, 21 (2013), pp.103-108 (in Japanese).

[11]Ushio K., Toyoda Y., Yamamoto N., Morita T. and Nakashima H., "Development of a Miniature Microwave Discharge Thruster", Trans. *JSASS Aerospace Tech. Japan*, Vol. 14, No. ists30, pp. Pb_141-Pb_147, 2016

[12]Ushio, K., Toyoda, Y., Yamamoto, N., Nakashima, H., "Performance Evaluation of a Miniature Microwave Discharge Thruster Considering Charge Exchange Collision", *Journal of IAPS*, Vol.2, No.1, 2015(in Japanese)

[13]Okuda, Y. Kusuda, M., Yamamoto, N., Morita, T. and Nakashima, H., "Internal physical analysis of Microwave Discharge Neutralizer with Full-PIC code", *Proceedings of 58th Space Sciences and Technology Conference*, JSASS-2015-4639, 2015(in Japanese)

[14]Yee, K. S.: Numerical Solution of Initial Boundary Value Problem Involving Maxwell's Equations in Isotopic Media, *IEEE Trans*. Antennas Propagat., 14 (1966), pp. 302–307.

[15]V. Vahedi and M. Surendra, "A Monte Carlo collision model for the particle-in-cell method: applications to argon and oxygen discharges", *Computer Physics Communications*, vol.87, pp.179-198,1995

[16]Funaki, I., Kuninaka, H., Toki, K.: Plasma Characterization of a 10-cm Diameter Microwave Discharge Ion Thruster, *Journal of Propulsion and Power*, 20 (2004), pp. 718-726.

[17]Ushio, K., Toyoda, Y., Yamamoto, N., Morita, T., Nakashima, H., "Plasma diagnostics of miniature microwave discharge plasma thruster", *Proceedings of 58th Space Sciences and Technology Conference*, Nov., 2014 (in Japanese).

[18]Ushio, K., Ueno, B., Yamamoto, N., Morita, T., Nakashima, H., "Potential Measurement of a Plasma and a Thruster in a Miniature Microwave Discharge Plasma Thruster", *Proceedings of the 8th Asian Joint Conference on Propulsion and Power*, AJCPP2016-166, 2016

[19]Kusuda, M., "Analysis of the extracted I-V characteristic in microwave discharge neutralizer", Master Thesis, Kyushu University, 2015(in Japanese).

[20]Masui, H., Tashiro, Y., Yamamoto, N., Nakashima, H., Funaki, I., "Analysis of Electron and Microwave Behavior in Microwave Discharge Neutralizer", *Trans. Japan Soc. Aero. Space Sci*., Vol. 49, No. 164, pp. 87–93, 2006

[21]Toyoda, Y., "Development of miniature microwave discharge thruster", Master's Thesis, Kyushu University, 2014(in Japanese).